Original article

Preoperative diagnosis of lymph node metastases in gastric cancer by magnetic resonance imaging with ferumoxtran-10

Yoshiaki Tatsumi[1], Nobuhiko Tanigawa[1], Haruto Nishimura[1], Eiji Nomura[1], Hideaki Mabuchi[1], Mitsuru Matsuki[2], and Isamu Narabayashi[2]

[1] Department of General and Gastroenterological Surgery, Osaka Medical College, 2-7 Daigaku-machi, Takatsuki, Osaka 569-8686, Japan
[2] Department of Radiology, Osaka Medical College, Osaka, Japan

Abstract

Background. Knowledge regarding the presence and location of lymph node metastasis in gastric cancer is essential in deciding on the operative approach. Lymph node metastases have been diagnosed with imaging tests such as computed tomography (CT) and ultrasonography (US); however, the accuracy of such diagnoses, based on size and shape criteria, has not been adequate. Ferumoxtran-10 (Combidex; Advanced Magnetics) is a lymphotropic contrast agent for magnetic resonance imaging (MRI) whose efficacy for the detection of metastatic lymph nodes in various cancers has been reported by several investigators; however, its efficacy for this purpose has not been reported for gastric cancer. We investigated the efficacy of ferumoxtran-10-enhanced MRI for the diagnosis of metastases to lymph nodes in gastric cancer.

Methods. Seventeen consecutive patients who were diagnosed with a nonearly stage of gastric cancer were enrolled in the study. All the patients were examined by MRI (Signa Horizon 1.5T; GE Medical; T2*-weighted images) before and 24h after the intravenous administration of ultrasmall particles of superparamagnetic iron oxide — ferumoxtran-10 (2.6 mg Fe/kg of body weight) — and the presence or absence of metastasis was determined from the enhancement patterns. The imaging results were compared with the corresponding histopathological findings following surgery.

Results. Of 781 lymph nodes dissected during surgery, the imaging results of 194 nodes could be correlated with their histopathological findings. Fifty-nine lymph nodes from 11 patients had histopathological metastases. In nonaffected normal lymph nodes, we observed dark signal intensity on MRI caused by the diffuse uptake of the contrast medium by macrophages resident in the lymph nodes, which phagocytose the iron oxide particles of ferumoxtran-10. The number of phagocytic macrophages was decreased in metastatic lymph nodes, and they showed various patterns of decreased uptake of ferumoxtran-10. Three enhancement patterns were observed in lymph nodes: (A) lymph nodes with overall dark signal intensity due to the diffuse uptake of ferumoxtran-10; (B) lymph nodes with partial high signal intensity due to partial uptake; and (C) no blackening of lymph nodes due to no uptake of ferumoxtran-10. Patterns (B) and (C) were defined as metastatic. The sensitivity, specificity, positive predictive value, negative predictive value, and overall predictive accuracy of postcontrast MRI were 100% (59/59), 92.6% (125/135), 85.5% (59/69), 100% (125/125), and 94.8% (184/194), respectively. These parameters for predictive accuracy were much superior to these parameters previously evaluated by CT or US. Nodes in the retroperitoneal and paraaortic regions were more readily identified and diagnosed on the MR images than those in the perigastric region.

Conclusion. The present study confirmed that ferumoxtran-10-enhanced MRI is useful in the diagnosis of metastatic lymph nodes and that the use of this modality will be helpful in treatment decision-making for gastric cancer patients.

Introduction

Lymph node dissection is essential in gastrointestinal carcinoma therapy, because adequate lymph node dissection of metastatic lymph nodes may give a better prognosis [1,2]. In gastric cancer patients the presence or absence of lymph node metastasis should be diagnosed precisely, prior to surgery, to allow selective lymph node dissection. Lymph node status has been evaluated prior to surgery using various imaging technologies, such as computed tomography (CT) and ultrasonography (US). The size or shape of the lymph nodes, and imaging patterns have been used as the standards for the diagnosis [3–5], but these methods have not been found to be sufficiently accurate.

As a result of the inability to accurately determine the status of lymph nodes before surgery, a wide extent of

lymph node dissection has been recommended for the surgical treatment of gastric cancers, regardless of the disease stage; for example, in the recent Japanese Gastric Cancer Association (JGCA) *Gastric cancer treatment guidelines* [6]. Some investigators have reported that sentinel node navigation surgery for early gastric cancer may provide promising results, but no consensus has been reached at present [7–9]. In addition, sentinel node evaluation may be unreliable, at least in patients with advanced gastric cancer, because lymphatic drainage patterns may be altered by cancer invasion.

Ferumoxtran-10 (Combidex; Advanced Magnetics, Cambridge, MA, USA) is a contrast agent for magnetic resonance imaging (MRI) consisting of ultrasmall superparamagnetic iron oxide (USPIO) particles which can contrast lymph nodes that have normally functioning macrophages. Ferumoxtran-10 has a smaller particle size which leads to its specific lymphotropic behavior than the clinically established superparamagnetic iron oxide (SPIO), Resovist (Schering Nordiska AB, Sweden), which is used clinically for the detection of liver tumors. When ferumoxtran-10 is administered intravenously, it is concentrated in the lymph nodes by direct transcapillary passage through high endothelial venules within the nodes and also by endothelial transcytosis from the systemic circulation into the interstitium, where it is drained to normally functioning lymph nodes [10]. The ferumoxtran-10 accumulated in lymph nodes markedly reduces the T2 signal intensity and is readily detectable by MRI.

Several investigators have reported the efficacy of ferumoxtran-10-enhanced MRI for the detection of metastatic lymph nodes of various cancers, including metastatic cervical lymph nodes of laryngeal cancer, axillary lymph nodes of breast cancer, and pelvic lymph nodes of prostate cancer or urinary bladder cancer, showing that the technique can be useful in these cancers [11–14]. However, in the peritoneal cavity, it is more difficult to obtain clear images of lymph nodes because of respiratory artifacts, and there are no reports so far on the detection of metastatic lymph nodes in cancers of intraabdominal organs.

Therefore, in this study, we evaluated the diagnostic accuracy of ferumoxtran-10 enhanced MR imaging in the lymph nodal staging of gastric cancer.

Patients and methods

Patients

The study was approved by the ethics committee at Osaka Medical College. From January 2004 to April 2005, 20 patients diagnosed with a nonearly stage of gastric cancer who were scheduled for curative surgery were enrolled. All patients were diagnosed with gastric cancer histologically by a biopsy via gastroendoscopy. Informed and written consent was obtained from all patients prior to the study. Multidetector-row helical CT (MDCT) imaging and MRI were performed before the intravenous administration of ferumoxtran-10. The lyophilized contrast agent was reconstituted and diluted in 100 ml of normal saline, and infused over a period of 60 min through a 5-μm filter, at a dose of 2.6 mg of iron per kilogram of body weight. Postcontrast MR imaging was taken 24–36 h after the contrast medium administration, using the same imaging sequences, planes, and parameters as those used in the precontrast study.

A dose of 2.6 mg of iron per kilogram was chosen on the basis of a phase II dose-ranging study and phase III results [11–15]. Adverse events for the enrolled patients were recorded from the time of administration of ferumoxtran-10 to surgery.

CT and MRI

MDCT images (Aquilion Multi scanner; Toshiba Medical Systems, Tokyo, Japan), obtained with 1-mm section thickness at 1-mm intervals, were reviewed in order to identify the location of lymph nodes. MDCT is a routine preoperative examination for all patients with gastric cancer at our department. All enrolled patients were examined by MRI (T2*-weighted images; Signa Horizon 1.5T; General Electric Medical Systems, Milwaukee, WI, USA), using a body coil, with the patient in the supine position, before and approximately 24 h after the intravenous administration of ferumoxtran-10. T2*-weighted gradient-recalled images were obtained with a 135/7.6–8.3(TR/TE) 60°flip angle, a 512×512 matrix, and 5-mm slice. Before MRI examination, patients had fasted for more than 3 hours. Scopolamine butylbromide (20 mg; Buscopan; Boehringer Ingelheim Japan, Kawanishi, Hyogo, Japan) was administered intramuscularly approximately 5 min before the MRI examination, unless it was contraindicated because of the patient's condition. The images were evaluated by two surgeons and one radiologist by consensus.

Diagnosis of lymph node metastasis

Multiple sections of all of the dissected lymph nodes were stained with hematoxylin and eosin, and the slides were reviewed by at least two experienced pathologists who had no knowledge of the MRI findings. The largest diameter of lymph nodes on each section was recorded. The anatomical locations of lymph nodes were identified on the MDCT images, and on precontrast T2*-weighted MR images as well. Quantitative diagnosis
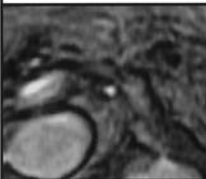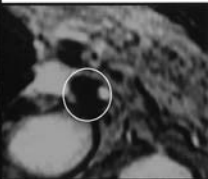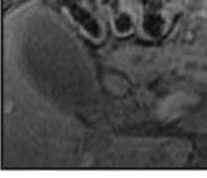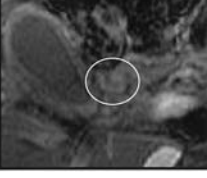
Fig. 1. Enhanced lymph node patterns with ferumoxtran-10. We subdivided the enhanced patterns of the lymph nodes into three categories: *A* nodes showing overall dark signal intensity due to the diffused uptake of ferumoxtran-10; *B* nodes showing partial high signal intensity due to partial uptake of ferumoxtran-10; and *C* noblackening of nodes due to absence of ferumoxtran-10 uptake. Patterns *B* and *C* were identified as metastatic. *MRI*, magnetic resonance imaging

was made on the postcontrast MR images. Three enhancement patterns of lymph nodes were observed: (A) lymph nodes with overall dark signal intensity due to diffuse uptake of ferumoxtran-10, (B) lymph nodes with partial high signal intensity due to partial uptake of ferumoxtran-10, and (C) no blackening of lymph nodes due to no uptake of ferumoxtran-10. In this study, patterns (B) and (C) were defined as metastatic (Fig. 1), while pattern (A) was nonmetastatic. Patterns of contrast were reviewed on postcontrast MR images. For the dissected lymph nodes whose anatomical locations were identified by CT or precontrast MR imaging, the histopathological findings were compared with the ferumoxtran-10 contrast patterns on MRI.

Statistical analysis

We categorized patterns (B) or (C) in metastatic lymph nodes as true positive; pattern (A) in nonmetastatic lymph nodes as true negative; patterns (B) or (C) in nonmetastatic lymph nodes as false positive, and pattern (A) in metastatic lymph nodes as false negative. Based on these findings, the sensitivity, specificity, positive predictive value, negative predictive value, and overall accuracy were calculated.

Results

Patient characteristics

Twenty patients who were initially scheduled for curative surgery for advanced gastric cancer underwent

MRI before and 24h after ferumoxtran-10 was administered. Two patients were subsequently excluded from this study, because of their far advanced stage of cancer, and were treated by chemotherapy instead of surgery. Another patient was found to have peritoneal metastasis at laparotomy, and gastrojejunostomy without lymph node dissection was performed. Consequently, 17 patients who were diagnosed with a nonearly stage of gastric cancer prior to surgery were enrolled.

There were 14 men (mean age, 59.8 years; range, 37–78 years) and 3 women (mean age, 68.3 years; range, 64–73 years). The mean age of all patients was 59 years (range, 52–75 years). No patient underwent preoperative chemotherapy or radiation therapy. Of the 17 patients, 2 had a stage T1 (TNM classification) tumor [16], 3 had a stage T2a tumor, 6 had stage T2b, 4 had stage T3, and 2 had a stage T4 tumor. The tumor histologies showed variable degrees of differentiation, from well-differentiated adenocarcinoma to signet-ring-cell carcinoma. Nine patients underwent distal gastrectomy; 6 total gastrectomy; 1 subtotal gastrectomy; and 1 pancreatoduodenectomy together with regional lymph node dissection. The mean interval between the ferumoxtran-10 enhanced MRI and the surgery was 3.6 days (range, 1–12 days).

Surgery

All 17 patients underwent primary tumor resection together with regional lymph node dissection, based on the *Gastric cancer treatment* guidelines [6]. Both group 1 and group 2 lymph nodes were systematically dissected, regardless of their MR images. By referring to the
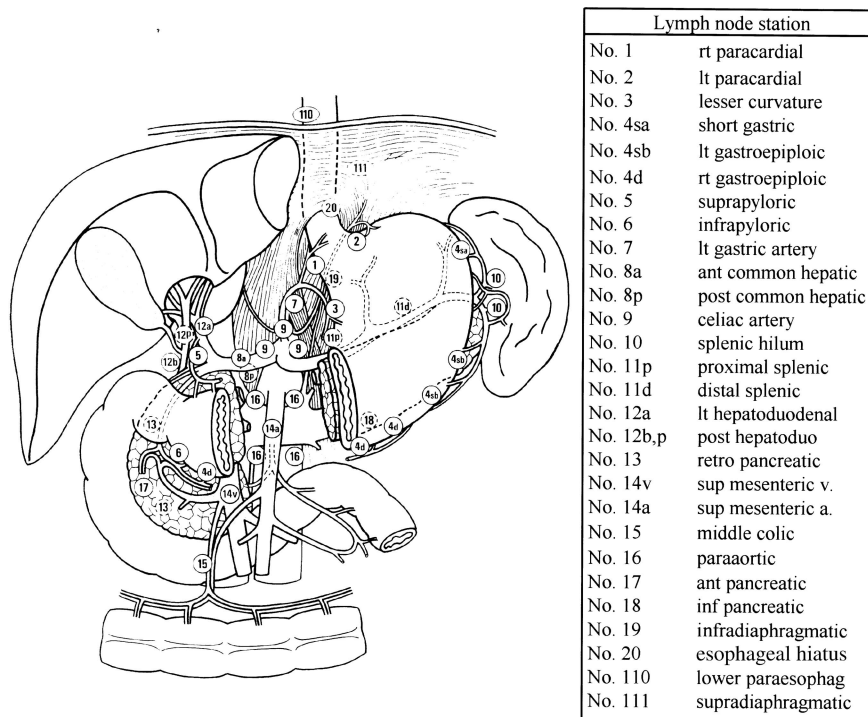
Lymph node station	
No. 1	rt paracardial
No. 2	lt paracardial
No. 3	lesser curvature
No. 4sa	short gastric
No. 4sb	lt gastroepiploic
No. 4d	rt gastroepiploic
No. 5	suprapyloric
No. 6	infrapyloric
No. 7	lt gastric artery
No. 8a	ant common hepatic
No. 8p	post common hepatic
No. 9	celiac artery
No. 10	splenic hilum
No. 11p	proximal splenic
No. 11d	distal splenic
No. 12a	lt hepatoduodenal
No. 12b,p	post hepatoduo
No. 13	retro pancreatic
No. 14v	sup mesenteric v.
No. 14a	sup mesenteric a.
No. 15	middle colic
No. 16	paraaortic
No. 17	ant pancreatic
No. 18	inf pancreatic
No. 19	infradiaphragmatic
No. 20	esophageal hiatus
No. 110	lower paraesophag
No. 111	supradiaphragmatic

Fig. 2. Lymph node stations modified from reference 17. *lt*, left; *rt*, right; *ant*, anterior; *post*, posterior; *sup*, superior; *v.*, vein; *a.*, artery; *inf*, inferior

Table 1. Characteristics of dissected lymph nodes

	n	Metastasis (+)	Metastasis (−)
Total no. of dissected lymph nodes	781	167	614
No. of lymph nodes identified by MRI	194	59	135
Diagnosed positive on MRI	69	59	10
Diagnosed negative on MRI	125	0	125
Size distribution of MRI nodes		Metastasis (+)	Metastasis (−)
Long-axis diameter (<5 mm)	66	8 (12.1%)	58 (87.9%)
Long-axis diameter (≧5, <10 mm)	86	28 (32.6%)	58 (67.4%)
Long-axis diameter (≧10 mm)	42	23 (54.8%)	19 (45.2%)

lymph-node images on ferumoxtran-10-enhanced MRI taken prior to surgery, were able to define the anatomical locations of some, but not all, lymph nodes.

The definition of the anatomical locations of regional lymph nodes around the stomach was based on the *Japanese classification of Gastric carcinoma* (JCGC) [17] (Fig. 2). Of 781 lymph nodes that were dissected during surgery (range, 9 to 82 nodes per patient), 194 nodes were identified on the MR images and their histopathological findings were compared with the corresponding contrast patterns on MR images on a node-by-node basis (range, 3 to 35 nodes per patient). The long-axis diameters of the dissected lymph nodes are listed in Table 1.

Safety evaluation

Patients were administered ferumoxtran-10 via a drip infusion lasting for over 60 min. Patients were observed closely for adverse events such as allergic skin changes or back pain. However, no adverse events were noted in this series of patients.

Diagnosis of lymph node metastasis by contrast patterns

A total of 781 lymph nodes in the 17 patients, including 167 metastatic lymph nodes, were dissected during surgery, and 194 of the 781 lymph nodes (24.8%) were

identified on the MR images and correlated with histopathological results. Of the 194 nodes, 59 contained metastatic deposits on pathological evaluation. The sensitivity, specificity, positive predictive value, negative predictive value, and overall accuracy of the postcontrast MR imaging were 100%, 92.6%, 85.5%, 100%, and 94.8%, respectively (Table 2). In the general clinical setting, on various imaging analyses, such as CT, US, and MRI, lymph nodes smaller than 10mm are assessed as normal, and those 10mm or larger are classified as enlarged lymph nodes. Using these size criteria to evaluate the identified nodes resulted in sensitivity, specificity, positive predictive value, negative predictive value, and overall accuracy of 38.9% (23/59), 85.9% (116/135), 54.8% (23/42), 76.3% (116/152), and 71.6% (139/194), respectively.

Of the above 167 metastatic lymph nodes, 38 (22.8%) were enlarged and 129 (77.2%) were normal-sized. Sixty-two (48.0%) of the 129 normal-sized nodes were

less than 5mm in size (Fig. 3). Of the 194 nodes for which the contrast patterns and their histopathological findings could be correlated, 59 lymph nodes from 11 patients had histopathological metastases. Of these metastatic lymph nodes, the long-axis diameter was less than 10mm in 36 nodes (61.0%). Of the 194 lymph nodes detected on MRI, 152 (78.4%) nodes were less than 10mm, including 36 metastatic nodes (23.7%), and 66 (34.0%) nodes were less than 5mm, including 8 metastatic nodes (12.1%). Of the 194 lymph nodes, 42 (21.6%) nodes were larger than or equal to 10mm, including 23 metastatic lymph nodes (54.8%). The sensitivity, specificity, positive predictive value, negative predictive value, and overall accuracy of postcontrast MRI in terms of size criteria are shown in Table 3.

Perigastric lymph nodes classified as group 1 (No. 1, 2, 3, 4, 5, and 6 lymph-node stations defined by the JCGC; shown in Fig. 2) were difficult to distinguish on MRI, mainly because of gastrointestinal peristalsis. In particular, most lymph nodes at the greater curvature could not be distinguished on MRI because of the presence of the neighboring transverse colon and its peristalsis. At the lesser curvature, it was hard to detect the lymph nodes, particularly those of normal size. In addition, the MR images were sometimes distorted by aortic motion artifacts, as can be seen in Fig. 4. Thus, the MR imaging patterns and histopathological findings could be correlated for only 44 (9.7%) of 454 dissected perigastric lymph nodes (including 110 metastatic lymph nodes). Of these 44 lymph nodes, 23 were true-positive nodes, 20 were true-negative nodes, and 1 (an infrapyloric node) was a false-positive node. The sensitivity, specificity, positive predictive value, negative predictive value, and overall accuracy of postcontrast MR imaging for these nodes were: 100% (23/23), 95.2% (20/21),
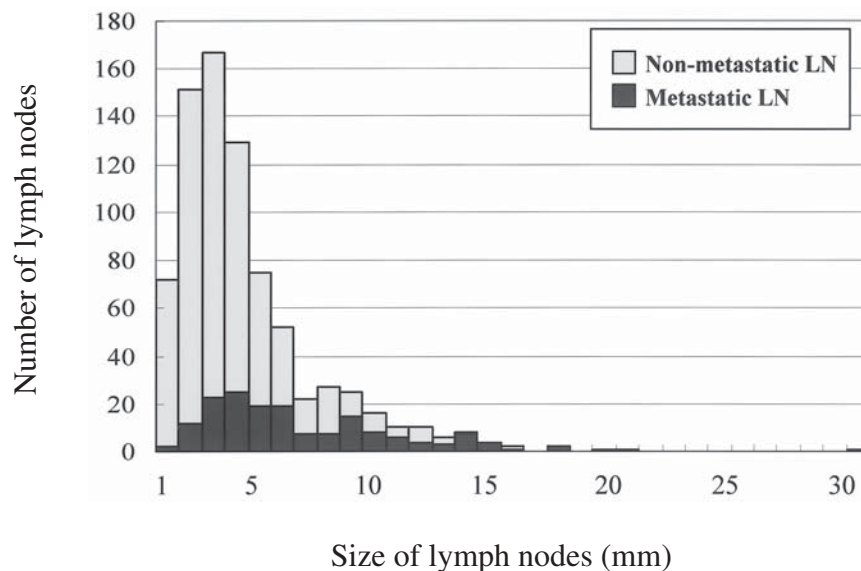
Table 2. Predictive accuracy of postcontrast MR imaging and a node-to-node comparison with histopathological findings for all of the dissected lymph nodes

MR imaging results	Histological metastasis (+)	Histological metastasis (−)	All nodes
Positive	59	10	69
Negative	0	135	135
Total	59	145	194

Positive results indicate metastatic nodes, and negative results indicate non-metastatic nodes. For ferumoxtran-10-enhanced MR imaging, the sensitivity was 100% (59/59); specificity, 92.6% (125/135); positive predictive value, 85.5% (59/69); and negative predictive value, 100% (125/125); accuracy was 94.8% (184/194)

Fig. 3. Sizes of the dissected lymph nodes. Of 167 metastatic lymph nodes detected among 781 dissected nodes, 38 (22.8%) nodes had an axis diameter of more than 10mm. Of the 781 dissected lymph nodes, 720 (92.2%) nodes, including 129 (17.9%) metastatic nodes, had an axis diameter less than 10mm; 519 (66.5%) nodes, including 62 (11.9%) metastatic nodes, had an axis diameter of less than 5mm; and 61 (7.8%) nodes, including 38 (62.2%) metastatic nodes, had an axis diameter greater than or equal to 10mm. *LN*, lymph node

Table 3. Predictive accuracy of postcontrast MR imaging based on the size criteria of lymph nodes

Long-axis diameter	TP	TN	FP	FN	Se	Sp	PPV	NPV	Acc
<5 mm	8	58	0	0	100% (8/8)	100% (58/58)	100% (8/8)	100% (58/58)	100% (66/66)
≧5, <10 mm	28	49	9	0	100% (28/28)	84.5% (49/58)	75.7% (28/37)	100% (49/49)	89.5% (77/86)
≧10 mm	23	18	1	0	100% (23/23)	94.7% (18/19)	95.8% (23/24)	100% (18/18)	97.6% (41/42)

TP, true positive; TN, true negative; FP, false positive; FN, false negative; Se, sensitivity; Sp, specificity; PPV, positive predictive value; NPV, negative predictive value; Acc, accuracy

Table 4. Predictive accuracy of enhanced MRI based on the anatomic regions of lymph nodes

Region	TP	TN	FP	FN	Se	Sp	PPV	NPV	Acc
Perigastric	23	20	1	0	100% (23/23)	95.2% (20/21)	95.8% (23/24)	100% (20/20)	97.7% (43/44)
Retro-peritoneal	30	80	6	0	100% (30/30)	93.0% (80/86)	83.3% (30/36)	100% (80/80)	94.8% (110/116)
Paraaortic	6	25	3	0	100% (6/6)	89.3% (25/28)	66.7% (6/9)	100% (25/25)	91.2% (31/34)

TP, true positive; TN, true negative; FP, false positive; FN, false negative; Se, sensitivity; Sp, specificity; PPV, positive predictive value; NPV, negative predictive value; Acc, accuracy
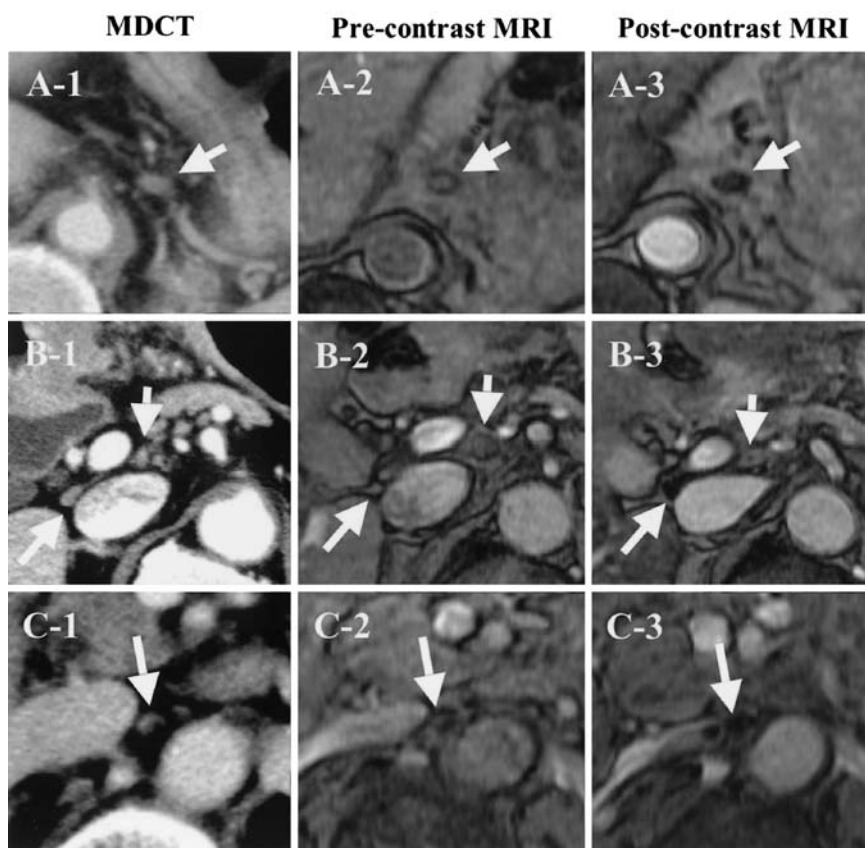

Fig. 4A–C. Clinical cases. **A** Perigastric lymph node; **B** retroperitoneal lymph node; **C** paraaortic lymph node; **A-1**, **A-2** Perigastric lymph node seen at the lesser curvature (No. 3; *arrows*) on multidetector-row helical computed tomography (MDCT) and precontrast MRI. **A-3** The signal intensity had decreased slightly on postcontrast MRI, but the node had not turned completely black (pattern B). This node was histopathologically diagnosed as a metastatic node. **B-1**, **B-2** A lymph node was seen posterior to the hepatoduodenal ligament (No. 12p; *long arrows*) on MDCT and precontrast MRI. **B-3** The node appeared completely black on post-contrast MRI and was histopathologically diagnosed as a normal node. **B-1**, **B-2** In addition, a lymph node was seen posterior to the common hepatic artery (No. 8p; *short arrows*) on MDCT and precontrast MRI. **B-3** However, the node did not appear black (pattern C) on post-contrast MRI and was histopathologically diagnosed as a metastatic node. **C-1**, **C-2** Paraaortic lymph nodes with unclear margins were observed on MDCT and pre-contrast MRI (No. 16; *arrows*). **C-3** These nodes appeared completely black on post-contrast MRI and were diagnosed as normal nodes

95.8% (23/24), 100% (20/20), and 97.7% (43/44), respectively (Table 4). In the 410 perigastric lymph nodes that were not identified by MR imaging, 87 were positive for metastasis.

The lymph nodes classified to group 2 (No. 7, 8, 9, 10, 11, 12, 14v lymph node stations defined by the JCGC, shown in Fig. 2) are located in the retroperitoneum, and thus the MR images of these retroperitoneal lymph nodes were less influenced by respiratory motion artifacts than the perigastric lymph nodes, and they were able to be identified more clearly. Information on group 2 lymph-node metastasis is helpful in surgical decision-making, including decisions on the extent of lymph-node dissection. In 116 (42.8%) of the 271 dissected group 2 lymph nodes, including 51 metastatic lymph nodes, contrast patterns on MRI were compared with

the corresponding histopathological findings. Of these 116 lymph nodes, 30 there true-positive nodes, 80 were true-negative nodes, and 6 were false-positive nodes. The sensitivity, specificity, positive predictive value, negative predictive value, and overall accuracy of postcontrast MRI in this group of nodes were: 100% (30/30), 93.0% (80/86), 83.3% (30/36), 100% (80/80), and 94.8% (110/116), respectively (Table 4). For the remaining 155 lymph nodes, the MRI and histopathological findings could not be compared, and 21 of these 155 lymph nodes were positive for metastases.

Metastatic lymph nodes around the abdominal aorta (No. 16 lymph node station defined by the JCGC, shown in Fig. 2) are defined as one parameter of distant metastasis (M1) by the TMN classification [16] for gastric cancer and defined as N3 or distant metastasis (M) by the JCGC. Survival is short for patients with these metastases, even after these nodes have been extensively dissected [18–20]. Therefore, identification of any metastatic lymph nodes in this station prior to surgery is important for determining the appropriate therapeutic strategy. Because the image quality of paraaortic lymph nodes, like that of lymph nodes in the retroperitoneal space, is not degraded by motion artifacts caused by respiration or gastrointestinal peristalsis, metastatic lymph nodes of rather small size could be identified. The smallest diameter of paraaortic lymph nodes that were identified in the present study was 3 mm for metastatic lymph nodes and 2 mm for normal lymph nodes. Ten of the 17 enrolled patients had lymph node dissection around the abdominal aorta. In 34 (60.7%) of the 56 dissected paraaortic lymph nodes (including 6 metastatic lymph nodes), contrast patterns on MRI were compared with the corresponding histopathological findings, while, for the remaining 22 lymph nodes, these findings could not be compared. Of the above 34 nodes, 6 were true-positive nodes, 25 were true-negative nodes, and 3 were false-positive nodes. The sensitivity, specificity, positive predictive value, negative predictive value, and overall accuracy of postcontrast MR imaging for thses nodes were: 100% (6/6), 89.3% (25/28), 66.7% (6/9), 100% (25/25), and 91.2% (31/34), respectively (Table 4). Of the 22 lymph nodes that could not be identified by MR images, none was found to have metastasis. In other words, this imaging diagnosis did not overlook any paraaortic lymph nodes positive for metastasis.

Discussion

No adverse events were observed in the patients who received ferumoxtran-10 administration in this study, although adverse events such as back pain or skin rash (range, 3%–28%) were reported in patients in previous studies [11–14]. In this study, ferumoxtran-10 was safely administered by drip infusion lasting for over 60 min at a dose of 2.6 mg Fe/kg.

To date, the presurgical diagnosis of lymph node metastasis from cancers of digestive organs has been done with CT images or ultrasonic tomography. The sizes and/or imaging patterns of the lymph nodes have been used as the standard for determination [1–3]. Some investigators define as metastatic those lymph nodes that are 1 cm or greater on CT images [2,3]. In our general clinical practice, we currently define lymph nodes as enlarged when the size is over 5 mm on CT images and as metastatic when nodes are over 10 mm. However, of the 781 dissected lymph nodes in the present study, 720 nodes were less than 10 mm in size and 129 (17.9%) of them were metastatic histologically. Of the 61 remaining dissected lymph nodes larger than or equal to 10 mm in size, metastases were confirmed histologically in 38 lymph nodes (62.3%). Although there were indeed some metastatic lymph nodes less than 10 mm in size, the incidence of metastasis was much higher for lymph nodes larger than or equal to 10 mm, as indicated in Fig. 3. However, when lymph nodes larger than or equal to 10 mm in size were diagnosed as metastatic by the customary size criteria, the sensitivity, specificity, positive predictive value, negative predictive value, and overall accuracy were 38.9% (23/59), 85.9% (116/135), 54.8% (23/42), 76.3% (116/152), and 71.6% (139/194), respectively. Thus, evaluation of the lymph node status based on the size criteria is not accurate enough to define lymph node status (N-stage). Bhandari et al. [21] described the overall sensitivity, specificity, and accuracy of MDCT for the N-staging of gastric cancer as 57.4%, 89.3%, and 75%. And Liao et al. [22] reported the overall sensitivity, specificity, and accuracy of abdominal ultrasonography for the N-staging of gastric cancer as 64.1%, 72.6%, and 77.6%. Our results with ferumoxtran-10-enhanced MRI were much superior to the results in these two reports.

MRI technology is constantly advancing: MRI with increasing signal intensities with strong magnetic fields, in which free breathing is used, and which is fast and silent is rapidly coming into common use. If the image quality and interpretation time achieved with MRI is similar to that achieved with MDCT, it can be expected that even more useful information would be obtained with ferumoxtran-10-enhanced MRI. Currently, among the popular diagnostic imaging tools, MDCT imaging has the best image quality. Increased detection of enlarged lymph nodes is achieved on MDCT with thin slices of 1 mm, and the anatomical location of lymph nodes can be identified precisely by three-dimensional construction (3D-CT), using a volume-rendering computer workstation (zioM900 Version 2; ZIO software, Tokyo, Japan) [23]. The combination of high-resolution

3D-CT with the diagnosis of lymph node metastasis by ferumoxtran-10-enhanced MRI could provide much useful information regarding lymph node metastasis.

In our study, of the 781 dissected lymph nodes, the number of nodes identified on MRI was 194. In regard to size distribution, the percentage of lymph nodes identified on MRI with a size less than 5mm was 12.7% (66/519), for those larger than or equal to 5mm, it was 42.8% (86/201), and for those larger than or equal to 10mm, it was 68.9% (42/61). That is to say, smaller lymph nodes are difficult to detect on MRI due to the limited resolution of MRI. In future, newly available high-resolution MRI will improve the results for the detection of smaller lymph nodes.

In our study, there were ten false-positive lymph nodes (Table 2). Deserno et al. [14] noted that several pathological changes in lymph nodes, including focal lipomatosis, focal fibrosis of nodal tissue, hilar fat, and reactive hyperplasia might be associated with such a false-positive evaluation.

The clinical significance of lymph node dissection for patients with gastric cancer is still controversial [24–26]. However, several studies, including our previous reports [27,28], have indicated that lymph node metastasis is an important prognostic factor for T2 gastric cancer. In addition, Hartgrink et al. [2] reported the prognostic significance of extended lymph node dissection for patients with N2 metastasis. Our present study has indicated that the detection of metastatic lymph nodes using ferumoxtran-10-enhanced MRI is an effective method of identifying group 2 and group 3 lymph-node metastases (N2, N3, or M defined by the JCGA), and may provide a rationale for surgical treatment with selective lymph node dissection.

In conclusion, the present study clearly showed that ferumoxtran-10-enhanced MRI enabled us to correctly evaluate the status of each lymph node around the primary gastric cancer. Such precise N-stage information will allow us to avoid unnecessary extended lymph node dissection in the surgical treatment of gastric cancer, which may, in turn, decrease subsequent patient morbidity and mortality,

References

1. Kodama Y, Sugimachi K, Soejima K, Matsusaka T, Inokuchi K. Evaluation of extensive lymph node dissection for carcinoma of the stomach. World J Surg 1981;5:241–8.
2. Hartgrink HH, van de Velde CJ, Putter H, Bonenkamp JJ, Klein Kranenbarg E, Songun I, et al. Extended lymph node dissection for gastric cancer: who may benefit? Final results of the randomized Dutch Gastric Cancer Group trial. J Clin Oncol 2004;22: 2069–77.
3. Fukuya T, Honda H, Hayashi T, Kaneko K, Tateshi Y, Ro T, et al. Lymph-node metastases: efficacy for detection with Helical CT in patients with gastric cancer. Radiology 1995;197:705–11.
4. Ogawa K, Hirai M, Katsune T, Miura K, Wakasugi S, Watanabe T, et al. Diagnosing ability of CT on periaortic lymph node metastasis of gastric cancer. J Jpn Clin Surg Soc 1994;55:843–7.
5. Nomura E, Okajima K, Isozaki H, Nakata E, Takeda Y, Ichinona T, et al. Studies of the metastatic lymph node and its images on computed tomography (CT) in gastric cancer. J Jpn Soc Clin Surg 1996;57:782–7.
6. Nakajima T. Gastric cancer treatment guidelines in Japan. Gastric Cancer. 2002;5:1–5.
7. Kitagawa Y, Fujii H, Mukai M, Kubota T, Otani Y, Kitajima M. Radio-guided sentinel node detection for gastric cancer. Br J Surg 2002;89:604–8.
8. Miwa K, Kinami S, Taniguchi K, Fushida S, Fujimura T, Nonomura A. Mapping sentinel nodes in patients with early-stage gastric carcinoma. Br J Surg 2003;90:178–82.
9. Isozaki H, Kimura T, Tanaka N, Satoh K, Matsumoto S, Ninomiya M, et al. Esophagus Gastrointestinal Surgical Treatment Study Group. An assessment of the feasibility of sentinel lymph node-guided surgery for gastric cancer. Gastric Cancer 2004;7:149–53.
10. Weissleder R, Elizondo G, Wittenberg J, Rabito CA, Bengele HH, Josephson L. Ultrasmall superparamagnetic iron oxide: characterization of a new class of contrast agents for MR imaging. Radiology 1990;175:489–93.
11. Harisinghani MG, Barentsz J, Hahn PF, Deserno WM, Tabatabaei S, van de Kaa CH, et al. Noninvasive detection of clinically occult lymph-node metastases in prostate cancer. N Engl J Med 2003;348:2491–9. Erratum in: N Engl J Med 2003;349: 1010.
12. Anzai Y, Piccoli CW, Outwater EK, Stanford W, Bluemke DA, Nurenberg P, et al. Evaluation of neck and body metastases to nodes with ferumoxtran 10-enhanced MR imaging: phase III safety and efficacy study. Radiology 2003;228:777–88.
13. Harisinghani MG, Dixon WT, Saksena MA, Brachtel E, Blezek DJ, Dhawale PJ, et al. MR lymphangiography: imaging strategies to optimize the imaging of lymph nodes with ferumoxtran-10 (review). Radiographics 2004;24:867–78.
14. Deserno WM, Harisinghani MG, Taupitz M, Jager GJ, Witjes JA, Mulders PF, et al. Urinary bladder cancer: preoperative nodal staging with ferumoxtran-10-enhanced MR imaging. Radiology 2004;233:449–56.
15. Hudgins PA, Anzai Y, Morris MR, Lucas MA. Ferumoxtran-10, a superparamagnetic iron oxide as a magnetic resonance enhancement agent for imaging lymph nodes: a phase 2 dose study. AJNR Am J Neuroradiol 2002;23:649–56.
16. International Union against Cancer. Sobin LH, Wittekind Ch. TNM classification of malignant tumors. 5th ed. Heidelberg Berlin Tokyo New York: Springer-Verlag; 1997.
17. Japanese Gastric Cancer Association. Japanese classification of gastric carcinoma, 2nd English edition. Gastric Cancer 1998;1: 10–24.
18. Takahashi S. Study of para-aortic lymph node metastasis of gastric cancer subjected to superextensive lymph node dissection. Nippon Geka Gakkai Zasshi (J Jpn Surg Soc) 1990;91:29–35.
19. Kitamura M, Arai K, Iwasaki Y. Clinicopathological studies and problems of para-aortic lymph node dissection: D4 dissection. Nippon Geka Gakkai Zasshi (J Jpn Surg Soc) 1996;97:302–7.
20. Isozaki H, Okajima K, Fujii K, Nomura E, Izumi N, Mabuchi H, et al. Effectiveness of paraaortic lymph node dissection for advanced gastric cancer. Hepatogastroenterology 1999;46:549–54.
21. Bhandari S, Shim CS, Kim JH, Jung JS, Cho JY, Lee JS, et al. Usefulness of three-dimensional, multidetector row CT (virtual gastroscopy and multiplanar reconstruction) in the evaluation of

gastric cancer: a comparison with conventional endoscopy, EUS, and histopathology. Gastrointest Endosc 2004;59:619–26.

22. Liao SR, Dai Y, Huo L, Yan K, Zhang L, Zhang H, et al. Transabdominal ultrasonography in preoperative staging of gastric cancer. World J Gastroenterol 2004;10:3399–404.

23. Lee SW, Shinohara H, Matsuki M, Okuda J, Nomura E, Tanigawa N, et al. Preoperative simulation of vascular anatomy by three-dimensional computed tomography imaging in laparoscopic gastric cancer surgery. J Am Coll Surg 2003;197:927–36.

24. Cuschieri A, Weeden S, Fielding J, Bancewicz J, Craven J, Joypaul V, et al. Patient survival after D1 and D2 resections for gastric cancer: long-term results of the MRC randomized surgical trial. Surgical Co-operative Group. Br J Cancer 1999;79:1522–30.

25. Bonenkamp JJ, Hermans J, Sasako M, van de Velde CJ. Extended lymph-node dissection for gastric cancer. Dutch Gastric Cancer Group. N Engl J Med 1999;340:908–14.

26. Roukos DH, Lorenz M, Encke A. Evidence of survival benefit of extended (D2) lymphadenectomy in western patients with gastric cancer based on a new concept: a prospective long-term follow-up study. Surgery 1998;123:573–8.

27. Isozaki H, Fujii K, Nomura E, Mabuchi H, Nishiguchi K, Tanigawa N. Prognostic factors of advanced gastric carcinoma without serosal invasion (pT2 gastric carcinoma). Hepatogastroenterology 1999;46:2669–72.

28. Komatsu S, Ichikawa D, Kurioka H, Kan K, Shioaki Y, Ueshima Y. Prognostic and clinical evaluation of patients with T2 gastric cancer. Hepatogastroenterology 2005;52:965–8.